Topology Optimization with Polymorphic Uncertainties using Artificial Neural Networks

Steffen Freitag, Simon Peters, Philipp Edler, Günther Meschke
Institute for Structural Mechanics, Ruhr University Bochum, 44801, Bochum, Germany,
steffen.freitag@sd.rub.de, {simon.peters, philipp.edler, guenther.meschke}@rub.de

Abstract. In this paper, a topology optimization approach is presented, where uncertain load and material parameters are considered. The concept of compliance minimization, i.e. stiffness maximization, is applied based on a plane stress finite element formulation. In order to take uncertain structural load parameters and uncertain material behavior into account, the topology optimization is embedded into a reliability-based design optimization approach, where uncertain structural parameters and design variables are quantified as random variables, intervals and probability boxes (p-boxes). This allows to consider aleatory and epistemic uncertainties by means of polymorphic uncertainty models within the topology optimization. Solving optimization problems with random variables, intervals and p-boxes leads to a high computational effort, because the objective functions and constraints have to evaluated millions of times. To speed up the optimization process, the finite element simulation of the topology optimization is replaced by artificial neural networks. This includes not only the topology dependent maximal stresses and displacements of the structure, which are used as constraints, but also the material density distribution inside the design domain. An example is presented, where the material volume of a cantilever structure is minimized, considering interval uncertainty only, combinations of interval and stochastic uncertainty and also polymorphic uncertainty (p-boxes) for the load, the material parameters and the geometry of the structure.

Keywords: Topology Optimization, Intervals, Random Variables, Probability Boxes, Polymorphic Uncertainty, Artificial Neural Network

1. Introduction

Structural optimization is focused on the design of engineering structures using the construction material in an efficient way. Objectives are in general minimizing the self weight, maximizing the stiffness or balancing the stresses of all structural members. Beside these objectives, constraints with respect to the structural load bearing capacity (e.g. strength of materials) and the serviceability (e.g. maximal displacements) have to be considered. The design variables of structural optimization problems are either sizing or shape parameters defining the dimensions of the structural members (shape optimization) or information about the material distribution defining the topology of the structure (topology optimization), see e.g. (Bendsøe and Sigmund, 2004).

Topology optimization has been successfully applied to improve the design of many real world applications, such as in automotive (Cavazzuti et al., 2011) or aerospace (París et al., 2012). Due

to innovations in additive manufacturing, its relevance for complex industrial problems has greatly increased. However, in civil engineering the number of applications is limited (Beghini et al., 2014) owing to e.g. the conservative industry in consequence of high-cost combined with high risk projects or the low material cost compared to regular hourly wage rate of civil engineers and construction worker tend to a mentality of over-sized and quickly mounted structures. However, the global cement production is the third-largest source of anthropogenic emissions of carbon dioxide (Andrew, 2018), which could lead to increasing prices for cement-based materials such as concrete due to policy measures such as carbon taxes soon (Lin and Li, 2011). Topology optimization could be one of the promising tools for more ecologically and architecturally appealing buildings (Beghini et al., 2014; Naboni and Paoletti, 2018). In civil engineering, topology optimization of structures is challenging, because of low volume fractions requiring fine design resolutions (Baandrup et al., 2020), which may be hard to be manufactured especially for large scale structures. Often, multi objectives and multi constraints have to be considered. In addition to this, aleatory and epistemic uncertainties of structural parameters should be taken into account in order to get robust designs.

Reliability-based and robust design optimization approaches have been developed to capture stochastic structural parameters and stochastic design variables, see e.g. (Schuëller and Jensen, 2008) and (Valdebenito and Schuëller, 2010). This requires to define appropriate uncertainty measures, e.g. by means of mean values, standard deviations and quantile values, to evaluate the objective functions and uncertain constraints. In case of polymorphic uncertainties, the reliability-based design optimization approaches are extended, which means that the stochastic uncertainty measures have to be combined with non-stochastic uncertainty measures to evaluate the objective functions and constraints, e.g. by lower or upper bounds for intervals (Edler et al., 2019) or by credibility levels for fuzzy numbers, see e.g. (Mäck et al., 2019).

Topology optimization approaches under consideration of stochastic uncertainties can be performed in the framework of reliability-based topology optimization, see e.g. (López et al., 2016) or robust optimization, see e.g. (Lazarov et al., 2012). Approaches for interval uncertainties have been developed e.g. in (da Silva et al., 2019) and (Wang and Gao, 2020). In (da Silva et al., 2020), a comparison on stochastic (robust and reliability-based) and non-stochastic (intervals for worst case) topology optimization approaches is presented. In this paper, a topology optimization approach is introduced, where both, aleatory and epistemic uncertainties are considered by combining stochastic and non-stochastic uncertainty models by means of random variables, intervals and p-boxes within the concept of polymorphic uncertainty quantification.

Solving optimization problems with random variables, intervals and p-boxes leads to a high computational effort, because the objective functions and constraints have to be evaluated millions of times. In order to reduce the computational effort, the finite element simulation model of the topology optimization process is approximated by artificial neural networks. Several feedforward networks are trained sequentially to efficiently evaluate the stress and displacement constraints of the topology optimization problem. This approach is based on the multilevel surrogate modeling strategy for the objective function computation introduced in (Freitag et al., 2020). Moreover, a feedforward network with high dimensional output is trained to learn the dependency between the selected material volume fraction (area fraction for 2D problems) and the corresponding optimal topology by means of the material densities inside the design domain. This allows one to quickly predict the optimal topologies with the artificial neural network.

2. Topology optimization

The first concept in structural optimization known as topology optimization, dating back to 1988 (Bendsøe and Kikuchi, 1988), distributes the densities of the discretized design domain, based on the use of an artificial composite material. Since then many different approaches where investigated, see e.g. (Sigmund and Maute, 2013).

2.1. Compliance minimization

In this paper, the well developed concept of compliance minimization $\min_\rho : c(\rho)$ (stiffness maximization) is used, where the problem for a fixed design domain with multiple deterministic loading conditions ($i = 1, \ldots, N_i$ load cases) and a volume constraint takes the following form:

$$\min_{\rho} : c(\rho) = \sum_{i=1}^{N_i} \mathbf{u_i^T} \cdot \mathbf{K}(\rho) \cdot \mathbf{u_i} \tag{1}$$

$$s.t. \begin{cases} \mathbf{K}(\rho) \cdot \mathbf{u} = \mathbf{f} \\ V(\rho) = V_f \cdot V_0 \\ 0 < \rho_{min} \leq \rho_e \leq 1 \end{cases} \tag{2}$$

In Eqs. (1) and (2), $\mathbf{u}, \mathbf{f}$ and $\mathbf{K}$ are the global displacement vector, the global force vector and the global stiffness matrix, respectively. The material density vector ρ contains the relative material densities ρ_e of all finite elements $e = 1, \ldots, N_e$, where N_e is the number of finite elements. The relative material densities ρ_e are defined in $[0, 1]$, but a minimum relative density ρ_{min} is considered for numerical reasons. V_0 is the material volume of the complete design domain, and

$$V(\rho) = \sum_{e=1}^{N_e} V_e \cdot \rho_e \tag{3}$$

is the material volume of the optimized structure for a prescribed volume fraction V_f, where V_e is the volume of a finite element e.

The problem formulation in Eqs. (1) and (2) follows a density approach (Bendsøe and Sigmund, 2004; Bendsøe, 1989), hence the stiffness matrix $\mathbf{K}$ depends on the material density. This relation could be chosen with anisotropic rank 3 laminates, which leads to an optimal solution of the optimization problem in Eqs. (1) and (2), see e.g. (Allaire et al., 2019; Bendsøe and Sigmund, 2004) for details. But this solution contains many finite elements with intermediate densities between 0 and 1, which are difficult to manufacture. In order to force black-white solutions, the modified Solid Isotropic Material with Penalization (SIMP) approach is used to express this connection. With the SIMP approach, the modulus of elasticity of each finite element is computed by

$$E_e(\rho_e) = E_{min} + {\rho_e}^p (E_0 - E_{min}), \qquad \rho_e \in [0, 1] \tag{4}$$

where E_0 is the modulus of elasticity of the material, E_{min} is a small modulus of elasticity defined for numerical reasons to avoid singularities in the stiffness matrix and p is the penalization parameter

(Andreassen et al., 2011), which is chosen as $p = 3$ in this work. As a result, the compliance for a single load case is calculated element wise as

$$c(\rho_e) = \sum_{e=1}^{N_e} E_e(\rho_e) \cdot \mathbf{u}_e^T \cdot \mathbf{k}_0 \cdot \mathbf{u}_e \ , \tag{5}$$

where $\mathbf{u}_e$ is the element displacement vector and $\mathbf{k}_0$ is the element stiffness matrix for a unit modulus of elasticity ($E = 1$).

2.2. Topology optimization with interval load position

Most of the topology optimization approaches assume deterministic conditions for the input data, obviating the different sources of uncertainties, which may affect significantly the structural performance. In the classical design concepts, the uncertainty of loads and the structural resistance is considered by partial safety factors and worst case analyses. Compared to the safety factor concept, the required volume fraction of a structure can be reduced by the direct implementation of aleatory and epistemic uncertain parameters and design variables into the topology optimization process (López et al., 2016). For the consideration of these uncertainties in topology optimization, two main approaches have been developed, i.e. robust and reliability-based formulations (Lazarov et al., 2012; Thore et al., 2017).

In this work, a reliability-based formulation with polymorphic uncertain parameters is developed by combining the topology optimization with a reliability-based global optimization to consider probabilistic constraints. Within the previously described topology optimization approach, an interval load position $\overline{x}_F = [{}_l x_F, {}_u x_F]$ is taken into account as a set of independent deterministic load positions $x_{F_1}, \ldots, x_{F_i}, \ldots, x_{F_{N_i}}$, where all N_i load positions are defined to be placed between the lower interval bound $x_{F_1} \geq {}_l x_F$ and the upper interval bound $x_{F_{N_i}} \leq {}_u x_F$. In every topology optimization step, the N_i load positions are considered as independent load cases, which are solved and superposed for the sensitivity and compliance calculation (Sigmund, 2001). Therefore, the sensitivities in each finite element are calculated as

$$\frac{dc_e}{d\rho_e} = \sum_{i=1}^{N_i} -p \cdot {\rho_e}^{p-1} \cdot (E_0 - E_{min}) \cdot \mathbf{u}_{e,i}^T \cdot \mathbf{k}_0 \cdot \mathbf{u}_{e,i} \ . \tag{6}$$

3. Reliability-based topology optimization with polymorphic uncertain parameters

3.1. Polymorphic uncertain parameters

In structural optimization, it is distinguished between uncertain design variables and uncertain a priori parameters, see e.g. (Edler et al., 2019), which both may influence the objective function and the constraints of an optimization problem. Uncertain design variables of an objective function to be optimized, allows one to take tolerances or variability of the design variables into account. In general, a reference value of an uncertain design variable, e.g. the mean value, is defined to

be optimized, but each design realization results in an uncertain structural response. Whereas uncertain design variables are varied for solving an optimization problem, uncertain a priori parameters are constant during the optimization, i.e. they cannot be optimized, but they also lead to an uncertain structural response. Within the concept of polymorphic uncertainty modeling, a topology optimization approach is presented, where uncertain parameters are considered as random variables, intervals and p-boxes.

Random variables are quantified by stochastic distribution functions, e.g. lognormal distribution or Gaussian distribution, which are defined by a probability density function (PDF) and the corresponding cumulative distribution function (CDF). In this work, three stochastic a priori parameters are considered as random variables, the structural load F, the modulus of elasticity E and the yield strength f_y.

In addition to the interval load position $\overline{x}_F$ introduced as interval a priori parameter of the topology optimization in Section 2.2, an interval design variable is defined to quantify an imprecise width of the structure $\overline{b}$ within a 2D finite element formulation of the presented topology optimization approach. The interval width $\overline{b}$ is represented by a range with lower and upper bounds

$$\overline{b} = [{}_l b,\ {}_u b] \ . \tag{7}$$

The interval midpoint

$${}_m b = \frac{1}{2} \cdot ({}_l b + {}_u b) \tag{8}$$

is defined to be optimized and the interval radius

$${}_r b = \frac{1}{2} \cdot ({}_u b - {}_l b) \tag{9}$$

is kept constant during the optimization.

Combining random variables and intervals as inputs of a structural simulation results in p-box of the structural response, i.e. the quantities of interest such as the maximal von Mises stress $\overline{\sigma}_V$ and the maximal displacement $\overline{w}$, which are used to evaluate the constraints of the optimization problem. A p-box is defined as an imprecise random variable with a lower bound CDF (e.g. ${}_l F(\sigma_V)$, ${}_l F(w)$) and an upper bound CDF (e.g. ${}_u F(\sigma_V)$, ${}_u F(w)$), which leads to interval probabilities, see e.g. (Ferson et al., 2003). Here, the lower and upper bound CDFs of the resulting p-boxes are represented by empirical distributions obtained from Monte Carlo simulations, which are denoted as free p-boxes according to (Schöbi and Sudret, 2017). In addition to have polymorphic uncertainty only in the results, p-boxes can also be considered directly as uncertain inputs. In this case, parametric p-boxes (Schöbi and Sudret, 2017) are used, which are quantified by a bunch of random variables with interval distribution parameters, e.g. interval mean values.

3.2. Objective function and design variables

The topology optimization problem given by Eqs. (1) and (2) is based on the minimization of the compliance of a structure for a predefined volume fraction V_f. This means that for each realization of V_f, where $0 \leq V_f \leq 1$, an optimal material volume distribution $V(\rho)$ within the design domain volume V_0 is obtained, where the material density ρ_e of each finite element e is a design variable.

In order to minimize the material volume V of the structure, a reliability-based global optimization problem is formulated. Here, a 2D plane stress finite element formulation is used to solve the topology optimization problem, see Eqs. (1) and (2). The volume of the structure, i.e. the objective function to be minimized, is given by

$$\text{min:} \quad {}_mV(A_f, \overline{b}) = A_f \cdot A_0 \cdot {}_mb \tag{10}$$

$$\text{s.t.} \quad \begin{cases} g_1 = {}_uP_{f,lbc} - P_{f,lbc,ac} \leq 0 \\ g_2 = {}_uP_{f,ser} - P_{f,ser,ac} \leq 0 \ , \end{cases} \tag{11}$$

where A_f is the area fraction of the design domain area A_0 and $\overline{b}$ is the interval width of the plane. The first design variable A_f is deterministic defined in $0 \leq A_f \leq 1$ and the second design variable $\overline{b}$ is an interval with midpoint ${}_mb$ to be optimized and a fixed radius ${}_rb$ taking construction impressions into account. Because of the interval design variable $\overline{b}$, the volume of the structure $\overline{V}$ is also an interval.

Here, the midpoint ${}_mV$ of the interval volume $\overline{V}$ is defined as objective function, because an optimization problem with interval design variables cannot directly be solved, see e.g. (Edler et al., 2019). However, it can be seen in Eq. (10), that the optimization problem is linear, which means that also lower or upper bounds of $\overline{V}$ can be used as objective function, and that in this case, the optimum is completely defined by one of the two constraint limit states ($g_1 = 0$ or $g_2 = 0$) in Eq. (11).

3.3. Constraints

The first inequality constraint $g_1 \leq 0$ in Eq. (11) is defined according to the load bearing capacity limit state of the structure. Here, the upper bound of the interval failure probability of the structure with respect to the load bearing capacity ${}_uP_{f,lbc}$ is given as the upper bound (worst case) probability that the p-box of the von Mises stress $\overline{\sigma}_V$ is exceeding the stochastic distributed yield strength of the material f_y in at least one element of the structure. $P_{f,lbc,ac}$ is the accepted failure probability with respect to the load bearing capacity.

The second inequality constraint $g_2 \leq 0$ in Eq. (11) is defined according to the serviceability limit state of the structure. In this work, the upper bound of the interval failure probability of the structure with respect to the serviceability ${}_uP_{f,ser}$ is defined as the upper bound (worst case) probability that the p-box of the displacement $\overline{w}$ is exceeding a tolerated displacement w_{ac} in at least one node of the structural finite element model. $P_{f,ser,ac}$ is the accepted failure probability with respect to the serviceability.

3.4. Solution of the optimization problem

The reliability-based topology optimization problem with polymorphic uncertain parameters is solved by a particle swarm optimization algorithm (Kennedy and Eberhart, 1995). In each optimization step, the objective function and the constraints have to be evaluated for each particle of the swarm. In Figure 1, the computational scheme of the reliability-based topology optimization is shown.

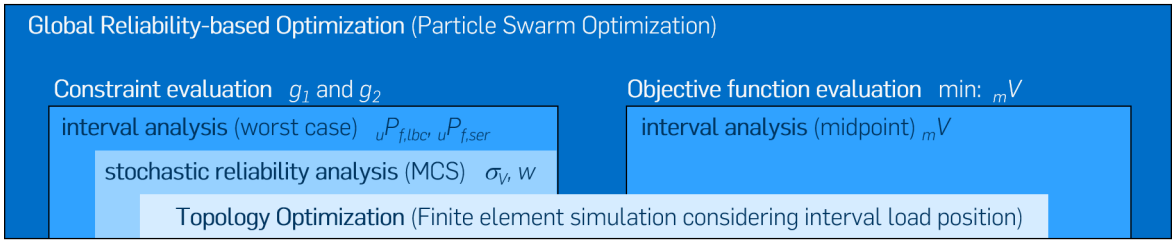

Figure 1. Computational scheme for reliability-based topology optimization.

The basis of the reliability-based topology optimization is the finite element based topology optimization presented in Section 2, which computes the optimal topology (element material densities $\rho_e(A_f)$), the maximal displacement $w^*(A_f)$ and the maximal von Mises stress $\sigma_V^*(A_f)$ for a selected area fraction A_f (deterministic design variable) and under consideration of an interval load position $\overline{x}_F$ (interval a priori parameter). It should be noted, that because of the linearity of the topology optimization problem, a scaled load F^*, a scaled modulus of elasticity E^* and a scaled width of the structure b^* is used for the finite element simulation to compute the scaled displacement w^* and the scaled von Mises stress σ_V^*. This allows one to use the FE results of one realization of the deterministic design variable A_f for the constraints evaluation and for the objective function evaluation by a simple post-processing of the FE results.

For the constraints evaluation, the p-box of the maximal von Mises stress is obtained by

$$\overline{\sigma}_V(A_f, \overline{b}) = \frac{F}{F^*} \cdot \frac{b^*}{\overline{b}} \cdot \sigma_V^*(A_f) \,, \tag{12}$$

and the p-box of the maximal displacement is computed by

$$\overline{w}(A_f, \overline{b}) = \frac{F}{F^*} \cdot \frac{b^*}{\overline{b}} \cdot \frac{E^*}{E} \cdot w^*(A_f) \,. \tag{13}$$

Equations (12) and (13) are solved by Monte Carlo Simulations (MCS) in combination with an interval analysis. Because of the monotonicity, it is sufficient to evaluate the lower bound ${}_l b$ of $\overline{b}$ within the interval analysis. Based on the results of Eqs. (12) and (13), the upper bound of the interval failure probability of the structure with respect to the load bearing capacity ${}_uP_{f,lbc} = P({}_u\sigma_V \leq f_y)$ and the upper bound of the interval failure probability of the structure with respect to the serviceability ${}_uP_{f,ser} = P({}_uw \leq w_{ac})$ and the corresponding values of the limit state functions g_1 and g_2 are computed by Eq. (11).

For the objective function evaluation, the midpoint ${}_mV$ of the interval volume $\overline{V}$ is computed by Eq. (10). In addition to the midpoint, also the corresponding interval volume can be determined by

$$\overline{V}(A_f, \overline{b}) = A_f \cdot A_0 \cdot \overline{b} \,, \tag{14}$$

where the interval bounds of $\overline{V}$ are obtained by interval arithmetic, i.e. by evaluating Eq. (14) for the lower and upper bounds of $\overline{b}$.

4. Artificial neural networks in topology optimization

The solution of the reliability-based topology optimization problem in Section 3 requires multiple runs of the finite element simulation based topology optimization with realizations of the deterministic design variable A_f to compute the element material densities $\rho_e(A_f)$ (deterministic topology design variables), and the corresponding maximal displacement $w^*(A_f)$ (serviceability constraint) as well as the maximal von Mises stress $\sigma_V^*(A_f)$ (load bearing constraint). In order to reduce the computation time, artificial neural networks are trained to approximate the finite element simulation.

4.1. Constraints approximation with artificial neural networks

For the computation of the maximal displacement $w^*(A_f)$ and the maximal von Mises stress $\sigma_V^*(A_f)$ two feedforward networks are generated based on finite element simulation results:

- ANN1_1: $A_f \mapsto \sigma_V^*$
- ANN2_1: $A_f \mapsto w^*$

Both networks ANN1_1 and ANN2_1 have one input neuron and one output neuron. The number of hidden layers and neurons are selected according to the complexity of the finite element simulation model, i.e. the topology optimization design domain. As can be seen in the example presented in Section 5, one hidden layer with a few neurons is sufficient to approximate a 2D plane stress finite element model for a rectangular design domain.

In order to further improve the performance of the optimization algorithm, two additional feedforward networks are generated based on results of ANN1_1 and ANN2_1:

- ANN1_2: $A_f, {}_m b \mapsto D_1\{g_1 = 0\}$
- ANN2_2: $A_f, {}_m b \mapsto D_2\{g_2 = 0\}$

ANN1_2 and ANN2_2 both have two inputs, the design variables A_f and ${}_m b$, and one output, which is the shortest distance $D_1\{g_1 = 0\}$ and $D_2\{g_2 = 0\}$ between a position in the design space and the constraint limit states $g_1 = 0$ and $g_2 = 0$, respectively. In order to compute the distances $D_1\{g_1 = 0\}$ and $D_2\{g_2 = 0\}$, the constraint limit states $g_1 = 0$ and $g_2 = 0$ are approximated by a space subdividing technique, see (Edler et al., 2019). The ANN-based distance function approximation allows one to efficiently move particles of the swarm, which are in the unfeasible region of the design space onto the constraint limit states, where the optimum of the linear optimization problem is located.

For all four artificial neural networks ANN1_1, ANN2_1, ANN1_2 and ANN2_2 the hyperbolic tangent activation function is used in the hidden neurons and the output neurons are activated by a linear activation function.

4.2. Topology prediction with artificial neural networks

In this work, an additional feedforward network is generated based on finite element simulation results to predict the optimal topology, i.e. the optimal material density ρ_e of each finite element e, for a given area fraction A_f:

– ANN3: $A_f \mapsto \rho_e$ with $e = 1, \ldots, N_e$

This ANN3 has one input A_f and a high dimensional (N-dimensional) output ρ_e, where the dimension N corresponds to the number of finite elements of the design domain. For such a high dimensional mapping, a deep neural network with several hidden layers and a lot of hidden neurons is required, see Section 5.

Because the material density is defined as $\rho_e \in [0, 1]$, the sigmoide activation function is used in all hidden neurons and also in the output neurons.

5. Example

In this section, a classical benchmark problem for topology optimization is presented to illustrate the described method for reliability-based topology optimization under consideration of polymorphic uncertainty. In Figure 2, the design domain (80 cm length and 25 cm height) and the boundary conditions of the investigated cantilever structure is shown. At the left boundary of the cantilever, the displacements are completely fixed and a vertically concentrated load $F^* = 10$ kN is applied at the top right side. The imprecise position of this vertical load is quantified as an interval $\overline{x}_F = [72, 80]$ cm with an interval width of 8 cm, see Figure 2.

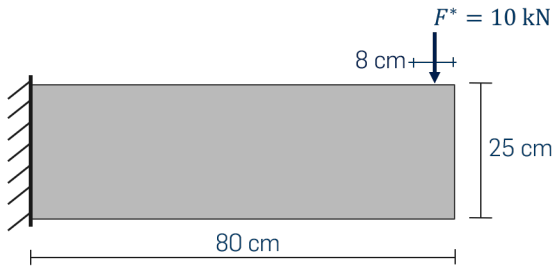

Figure 2. Design domain and boundary conditions for the topology optimization of a cantilever beam.

5.1. Finite element model for the topology optimization

For the finite element analysis of the cantilever, a structured mesh of 80 × 25 four-node bilinear square elements is used over the entire rectangular design domain, i.e. 2000 elements in total with dimensions 1 cm × 1 cm. Plane stress conditions and a width of $b^* = 1$ cm are selected. The whole structure is made of steel S235, therefore the elastic material is assumed to be linearly

isotropic with modulus of elasticity $E^* = 21000$ kN/cm^2, Poisson ratio $\nu = 0.3$ and yield strength $f_y^* = 23.5$ kN/cm^2.

The deterministic topology optimization problem according to Eq. (1) is solved for 65 discrete area fractions A_f in the range of 0.2 to 1.0, i.e. A_f is systematically reduced from 1.0 to 0.2 with a step size of $\Delta A_f = 0.0125$. It should be noted that the area fraction A_f is equivalent to the volume fraction V_f. The interval load position $\overline{x}_F$ is considered by evaluating Eq. (6) for $N_i = 9$ independent load cases. This means that the load is applied at nine different positions of the 8 cm wide loading zone and all 9 load positions are considered for the sensitivity and compliance calculation in each optimization step.

For the finite element simulations, an in house MATLAB code is used, which is based on (Andreassen et al., 2011). In the simulations, a sensitivity filter, where r_{min} is set to 3 cm, is used to prevent checkerboard patterns, see (Bendsøe and Sigmund, 2004) for details about filtering methods in general. For the 65 area fractions, the optimal topologies (final element material density ρ_e for each of the $N_e = 2000$ finite elements) and the corresponding maximal displacements w^* as well as the corresponding maximal von Mises stresses σ_V^* are stored.

5.2. Artificial neural network training

For ANN1$_1$ and ANN2$_1$, feedforward networks with one hidden layer comprising five hidden neurons are trained to approximate the dependencies between the area fraction A_f and the maximal von Mises stress $\sigma_V^*(A_f)$ as well as the dependencies between the area fraction A_f and the maximal displacement $w^*(A_f)$, respectively. Only 21 out of the 65 finite element simulation results have been used to set up the neural networks. Because it has been decided to restrict the design space for the area fraction A_f to the range of 0.2 to 0.7, the neural networks have only been trained for this range. In Figure 3, the neural network predictions are compared with finite element simulation results.

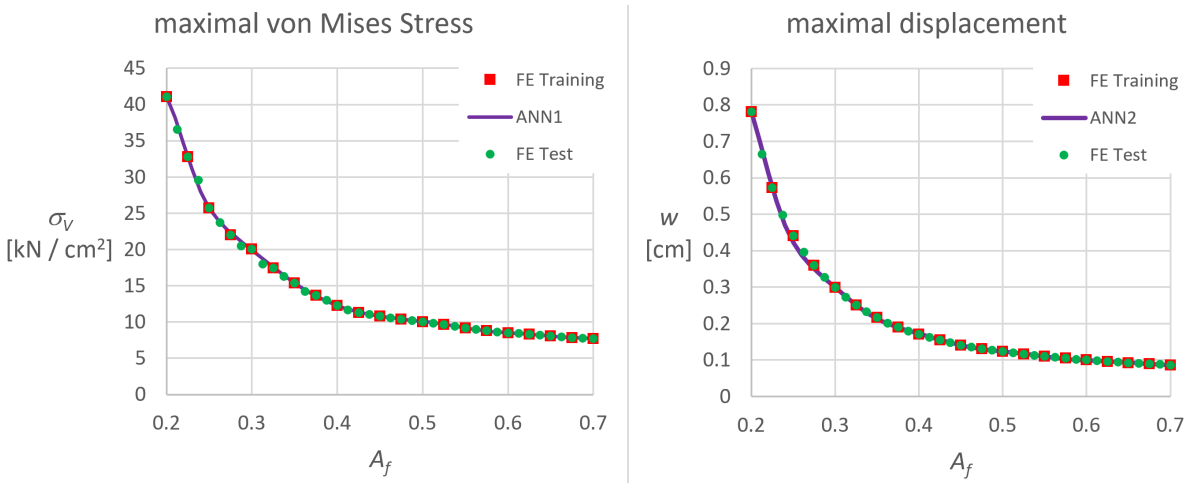

Figure 3. Comparison of ANN1$_1$ (left) and ANN2$_1$ (right) with finite element simulation results (FE) used for training and testing.

Using results of ANN1_1 and ANN2_1 in combination with Monte Carlo simulations to compute the failure probabilities with respect to the load bearing capacity and the serviceability, two additional artificial neural networks (ANN1_2 and ANN2_2) are trained to approximate the shortest distance to the constraint limit states $g_1 = 0$ and $g_2 = 0$, respectively. Also one hidden layer is sufficient for these networks, where the number of hidden neurons is 10 for ANN1_2 and 4 for ANN2_2.

In order to learn the optimal topology (the optimal material density distribution ρ_e of the structure) for specific area fractions A_f, an ANN3 is created, which has 2000 output neurons corresponding to the number of finite elements. For this challenging task, a deep feedforward neural network with three hidden layers and 1000 hidden neurons per layer is used.

It should be noted, that for all ANNs different architectures (with different numbers of hidden layers and hidden neurons) have been investigated and here only the finally used ANN architectures are described.

5.3. Results of the reliability-based topology optimization

The topology optimization is performed with different number of uncertain a priori parameters and finally also with an interval design variable. In order to investigate the influence of the uncertain parameters to the optimal design, three topology optimization problems are formulated according to the following parameters:

- **Problem 1**: optimization only with interval load position
  - deterministic design variables:
    - A_f
    - $\rho_e(A_f)$
    - b
  - uncertain a priori parameters:
    - $\overline{x}_F = [72, 80]$ cm (interval)
  - deterministic constraints:
    - $g_1 = \sigma_V^* - f_y^* \leq 0$
    - $g_2 = w^* - 0.3\ cm \leq 0$
- **Problem 2**: optimization with interval load position and stochastic a priori parameters
  - deterministic design variables:
    - A_f
    - $\rho_e(A_f)$
    - b
  - uncertain a priori parameters:
    - $\overline{x}_F = [72, 80]$ cm (interval)
    - F (normal distributed random variable with mean value $\mu(F) = 10$ kN and standard deviation $\sigma(F) = 2$ kN)

  - E (lognormal distributed random variable with mean value $\mu(E) = 21000$ kN/cm^2 and standard deviation $\sigma(E) = 1050$ kN/cm^2)
  - f_y (lognormal distributed random variable with mean value $\mu(f_y) = 23.5$ kN/cm^2 and standard deviation $\sigma(f_y) = 1.175$ kN/cm^2)
- stochastic constraints:
  - $g_1 = P_{f,lbc} - P_{f,lbc,ac} \leq 0$ (with $P_{f,lbc} = P(\sigma_V \leq f_y)$ and $P_{f,lbc,ac} = 7 \cdot 10^{-5}$)
  - $g_2 = P_{f,ser} - P_{f,ser,ac} \leq 0$ (with $P_{f,ser} = P(w \leq 0.3$ cm) and $P_{f,ser,ac} = 6.7 \cdot 10^{-2}$)

– **Problem 3**: optimization with interval load position, stochastic a priori parameters and interval design variable

- design variables:
  - A_f (deterministic)
  - $\rho_e(A_f)$ (deterministic)
  - $\overline{b}$ (interval, with midpoint ${}_m b$ to be optimized and fixed radius ${}_r b = 1$ mm)
- uncertain a priori parameters:
  - $\overline{x}_F = [72, 80]$ cm (interval)
  - F (normal distributed random variable with mean value $\mu(F) = 10$ kN and standard deviation $\sigma(F) = 2$ kN)
  - E (lognormal distributed random variable with mean value $\mu(E) = 21000$ kN/cm^2 and standard deviation $\sigma(E) = 1050$ kN/cm^2)
  - f_y (lognormal distributed random variable with mean value $\mu(f_y) = 23.5$ kN/cm^2 and standard deviation $\sigma(f_y) = 1.175$ kN/cm^2)
- interval-stochastic constraints:
  - $g_1 = {}_u P_{f,lbc} - P_{f,lbc,ac} \leq 0$ (with ${}_u P_{f,lbc} = P({}_u \sigma_V \leq f_y)$ and $P_{f,lbc,ac} = 7 \cdot 10^{-5}$)
  - $g_2 = {}_u P_{f,ser} - P_{f,ser,ac} \leq 0$ (with ${}_u P_{f,ser} = P({}_u w \leq 0.3$ cm) and $P_{f,ser,ac} = 6.7 \cdot 10^{-2}$)

It should be noted, that problem 3 is the general case, which has been described in Sections 2 and 3. Problem 1 and problem 2 are selected just for the comparison of the results. The uncertainty of the parameters is increased step by step from problem 1 to problem 3. The objective of all three optimization problems is the minimization of the midpoint ${}_m V$ of the required material volume $\overline{V}$ according to Eq. (10), where for problem 1 and problem 2, the required material volume is deterministic, i.e. ${}_m V = V$.

The three optimization problems are solved by particle swarm optimization using five particles. For the evaluation of the constraints and the prediction of the optimal topologies, the artificial neural network surrogate models are applied. In Figure 4, the results of the three optimization problems are presented, see also Table I. The optima are all placed at the constraint limit state functions, which are marked by continuous and dashed lines in Figure 4. The corresponding optimal topologies for the three optimization problems are shown in Figure 5. It can be seen, that the topology predictions based on the high dimensional artificial neural network ANN3 fit very good

with the results of the finite element (FE) simulations. Please note that these results were not used to train the ANN.

As expected, the midpoint ${}_mV$ of the required material volume is increasing with increasing uncertainty in order to guarantee robust designs. However, this is mainly achieved by increasing the midpoint of the width ${}_mb$ of the structure, because surprisingly the area fraction A_f is reduced for increasing uncertainty. One reason could be, that the sensitivities for the varying width of all finite elements are linear, due to the 2D formulation. Moreover lowering the area fraction A_f leads towards other optimized designs of the structure, i.e. only the densities of less important elements (elements with low sensitivities) are reduced to zero. It follows that the trailing optimization process first reduces the densities of all elements with less than linear sensitivities and supports all elements with higher than linear sensitivities.

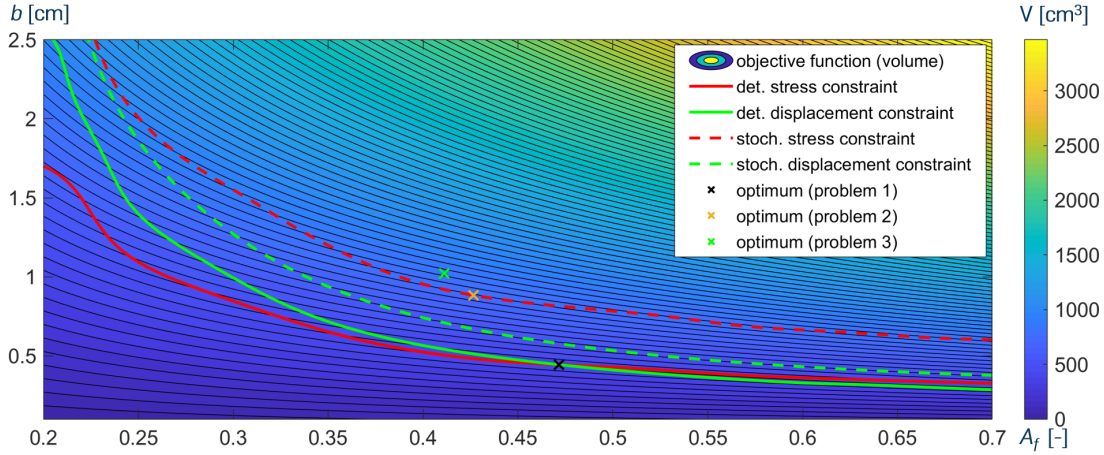

Figure 4. Optimal design variables of the area fraction A_f and the midpoint ${}_mb$ of the interval width of the structure, the three optima are obtained for optimization with interval load position (problem 1), with additional stochastic a priori parameters F, E and f_y (problem 2) and with the additional interval design variable $\overline{b}$ (problem 3).

Table I. Optima of the design variables A_f and ${}_mb$ and corresponding values of the objective function ${}_mV$

	problem 1	problem 2	problem 3
A_f [-]	0.47	0.43	0.41
${}_mb$ [cm]	0.44	0.88	1.02
${}_mV$ [cm^3]	419	753	839

An additional comparison of the results is done by removing the width of the structure (b or $\overline{b}$) from the design variables. This means that in this case, only the area fraction A_f and the element material density $\rho_e(A_f)$ are used as deterministic design variables. The white line in Figure 6 shows

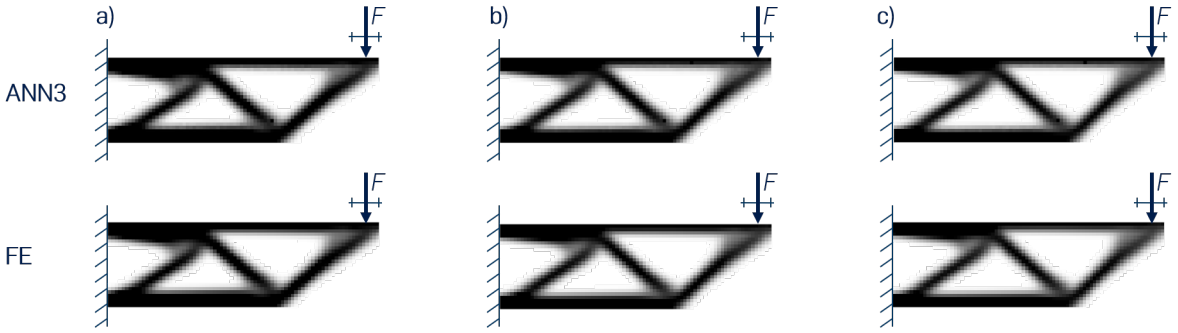

Figure 5. Optimal topologies predicted by an artificial neural network (ANN3) and comparison with finite element simulation (FE); a) interval load position (problem 1); b) with additional stochastic a priori parameters F, E and f_y (problem 2); c) with additional interval design variable $\overline{b}$ (problem 3).

this special case. It can now be seen, that, as expected, the area fraction A_f and consequently also the midpoint ${}_mV$ of the required material volume is increasing with increasing uncertainty, see also Table II and Figure 7.

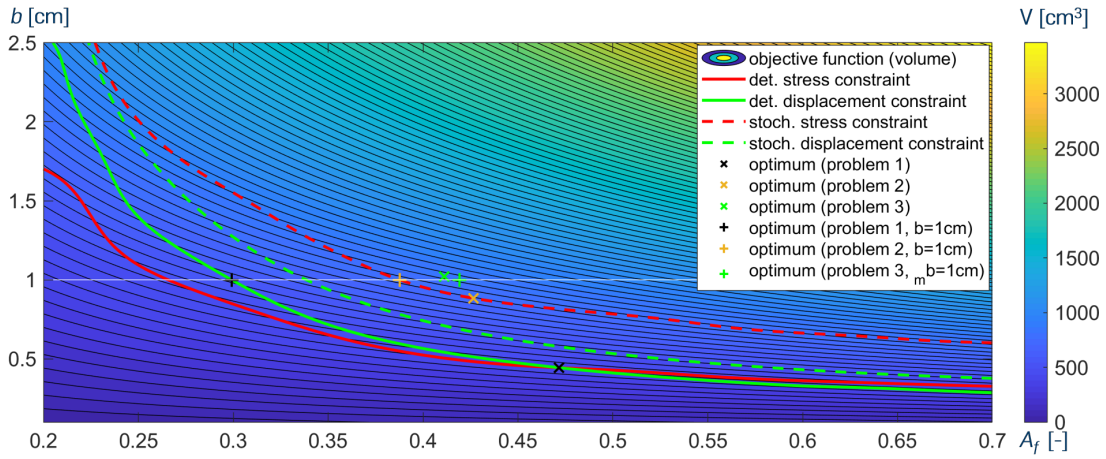

Figure 6. In addition to the results in Figure 4, the optimal area fraction A_f is evaluated for a constant structural width of $b = 1$ cm (for problem 1 and problem 2) and for $\overline{b} = [0.9, 1.1]$ cm (for problem 3), three additional results at the white line for optimization with interval load position only (problem 1), with additional stochastic a priori parameters F, E and f_y (problem 2) and with additional interval a priori parameter $\overline{b}$ (problem 3).

In the presented problems 2 and 3, intervals and random variables are used as uncertain parameters and the resulting maximal von Mises stresses and displacements are obtained as free p-boxes. This means, that the combination of intervals and random variables in the input space leads to polymorphic uncertain results and finally imprecise probabilities, which are used to evaluate the

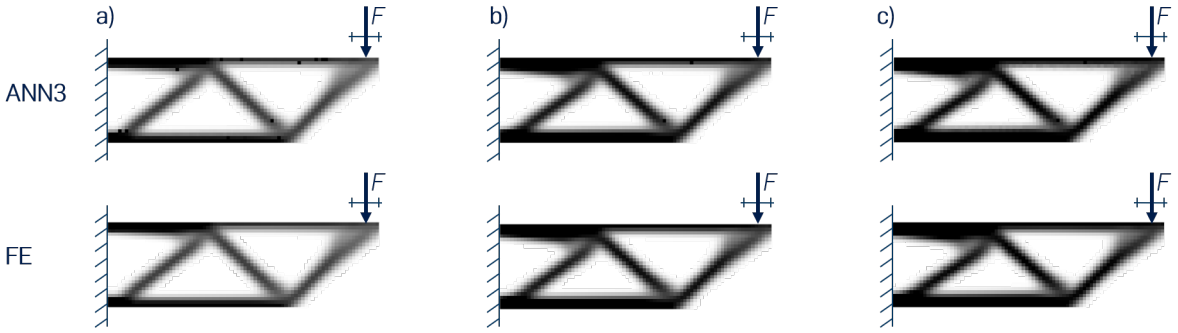

Figure 7. Optimal topologies predicted by an artificial neural network (ANN3) and comparison with finite element simulation (FE); a) interval load position; b) with additional stochastic a priori parameters F, E and f_y; c) with additional interval a priori parameter $\overline{b}$

Table II. Optima of the design variable A_f and the corresponding value of the objective function ${}_mV$ for a constant structural width $b = 1$ cm (for problem 1 and problem 2) and $\overline{b} = [0.9, 1.1]$ cm (for problem 3)

	problem 1	problem 2	problem 3
A_f [-]	0.30	0.39	0.42
${}_mV$ [cm^3]	598	775	838.5

failure probability constraints. However, the presented approach also works, if polymorphic uncertainty is already considered in the input space of the optimization problem. This is demonstrated by an additional problem 4, where the random variables of problems 2 and 3 are extended to parametric p-boxes quantified as normal and lognormal distributed random variables with interval mean values:

– **Problem 4**: optimization with interval load position, polymorphic uncertain a priori parameters defined as parametric p-boxes and interval design variable
  - design variables:
    * A_f (deterministic)
    * $\rho_e(A_f)$ (deterministic)
    * $\overline{b}$ (interval, with midpoint ${}_mb$ to be optimized and fixed radius ${}_rb = 1$ mm)
  - uncertain a priori parameters:
    * $\overline{x}_F = [72, 80]$ cm (interval)

  - $\overline{F}$ (normal distributed parametric p-box with mean value $\overline{\mu}(F) = [9.5, 10.5]$ kN and standard deviation $\sigma(F) = 2$ kN)
  - $\overline{E}$ (lognormal distributed parametric p-box with mean value $\overline{\mu}(E) = [20750, 21250]$ kN/cm^2 and standard deviation $\sigma(E) = 1050$ kN/cm^2)
  - $\overline{f}_y$ (lognormal distributed parametric p-box with mean value $\overline{\mu}(f_y) = [23.2, 23.8]$ kN/cm^2 and standard deviation $\sigma(f_y) = 1.175$ kN/cm^2)
- interval-stochastic constraints:
  - $g_1 = {}_uP_{f,lbc} - P_{f,lbc,ac} \leq 0$ (with ${}_uP_{f,lbc} = P({}_u\sigma_V \leq f_y)$ and $P_{f,lbc,ac} = 7 \cdot 10^{-5}$)
  - $g_2 = {}_uP_{f,ser} - P_{f,ser,ac} \leq 0$ (with ${}_uP_{f,ser} = P({}_uw \leq 0.3$ cm) and $P_{f,ser,ac} = 6.7 \cdot 10^{-2}$)

The results of problem 4 are shown in Table III and Figure 8. Compared to the results of problems 1 to 3, it can be seen, that the midpoint ${}_mV$ of the required material volume is further increasing because of the additional interval uncertainty of the stochastic distribution parameters.

Table III. Optima of the design variables A_f and ${}_mb$ and the corresponding value of the objective function ${}_mV$ of problem 4

	optimization with two design variables	optimization with one design variable and constant width $\overline{b} = [0.9, 1.1]$ cm
A_f [-]	0.42	0.44
${}_mb$ [cm]	1.05	1.0
${}_mV$ [cm^3]	872	874

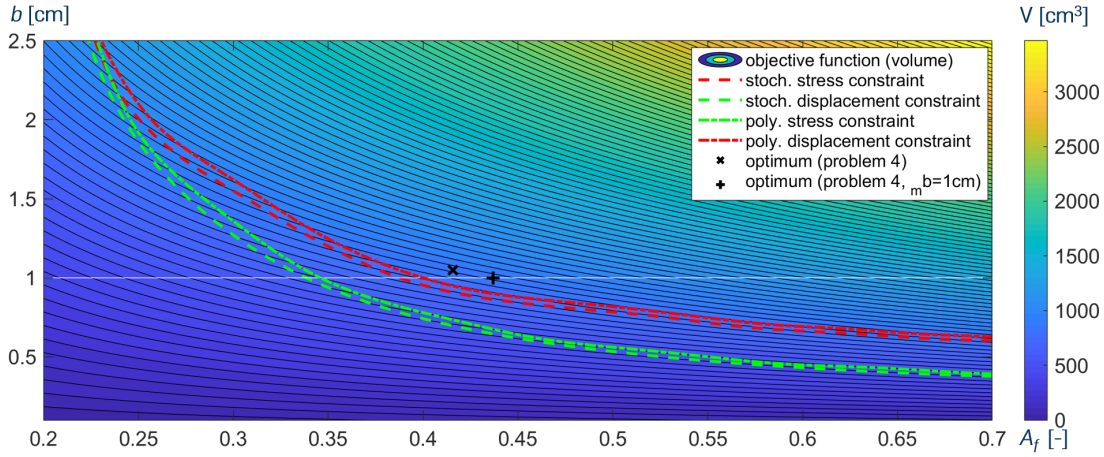

Figure 8. Optimal design variable of the area fraction A_f and the midpoint ${}_mb$ of the interval width of the structure for problem 4, the result at the white line shows the optimal area fraction A_f evaluated for a constant structural width of $\overline{b} = [0.9, 1.1]$ cm.

6. Conclusion

In the paper, a reliability-based topology optimization approach has been presented, where intervals, random variables and p-boxes are considered by means of a polymorphic uncertainty quantification. The finite element based topology optimization has been embedded into a structural optimization approach in order to consider probabilistic constraints (accepted failure probabilities) with respect to the structural load bearing capacity and the serviceability. The results of a cantilever structure optimization have shown, that as expected for increasing uncertainty, more material volume is required. But surprisingly, only the width of the structure is increased and the area fraction is reduced with increasing uncertainty. This can partially be explained by the sensitivities used within the compliance minimization, but needs further investigation in future works.

In order to reduce the numerical effort, several artificial neural networks have been trained to approximate the constraints evaluation as well as the optimal topology computation. Whereas for the constraint approximations small ANN architectures are sufficient, a deep ANN with 2000 output neurons has been created to predict the material density of each finite element in the design domain for a specific area (volume) fraction. Also if the example presented in this paper is an academic one, the potential of deep ANNs for topology prediction has been demonstrated. In future works, the concept of ANN-based topology prediction can be extended to 3D problems and to speed up the finite element simulation also during the topology optimization process, i.e. not only to predict the final optimal topology for a given volume fraction but also the sequential compliance minimization process. It is also planned to perform sensitivity analyses of the uncertain input parameters and to systematically investigate the consequence of FE discretization and ANN training errors, as well as minimization residuals of the optimization approach to the results.

Acknowledgements

This research is funded by the Deutsche Forschungsgemeinschaft (DFG, German Research Foundation) – Project number: 312921814 within Subproject 6 of the Priority Programme SPP 1886 "Polymorphic uncertainty modelling for the numerical design of structures".

References

Allaire, G., P. Geoffroy-Donders, and O. Pantz. Topology optimization of modulated and oriented periodic microstructures by the homogenization method. *Computers & Mathematics with Applications*, 7:2197–2229, 2019.

Andreassen, E., A. Clausen, M. Schevenels, B. S. Lazarow, and O. Sigmund. Efficient topology optimization in MATLAB using 88 lines of code. *Structural and Multidisciplinary Optimization*, 43:1–16, 2011.

Andrew, R. M. Global CO_2 emissions from cement production. *Earth System Science Data*, 10:195–217, 2018.

Baandrup, M., O. Sigmund, H. Polk, and N. Aage. Closing the gap towards super-long suspension bridges using computational morphogenesis. *Nature Communications*, 11:2735, 2020.

Beghini, L. L., A. Beghini, N. Katz, W. F. Baker, and G. H. Paulino. Connecting architecture and engineering through structural topology optimization. *Engineering Structures*, 59:716–726, 2014.

Bendsøe, M. P. and O. Sigmund. *Topology Optimization*. Springer, Berlin Heidelberg New York, 2004.

Bendsøe, M. P. and N. Kikuchi. Generating optimal topologies in structural design using a homogenization method. *Computer Methods in Applied Mechanics and Engineering*, 71:197–224, 1988.

Bendsøe, M. P.. Optimal shape design as a material distribution problem. *Structural Optimization*, 1:193–202, 1989.

Cavazzuti, M., A. Baldini, E. Bertocchi, D. Costi, E. Torricelli, and P. Moruzzi. High performance automotive chassis design: a topology optimization based approach. *Structural and Multidisciplinary Optimization*, 44:45–56, 2011.

da Silva, G. A., E. L. Cardoso, and A. T. Beck. Non-probabilistic robust continuum topology optimization with stress constraints. *Structural and Multidisciplinary Optimization*, 59:1181–1197, 2019.

da Silva, G. A., E. L. Cardoso, and A. T. Beck. Comparison of robust, reliability-based and non-probabilistic topology optimization under uncertain loads and stress constraints. *Probabilistic Engineering Mechanics*, 59:103039, 2020.

Edler, P., S. Freitag, K. Kremer, and G. Meschke. Optimization Approaches for the Numerical Design of Structures under Consideration of Polymorphic Uncertain Data. *ASCE-ASME Journal of Risk and Uncertainty in Engineering Systems Part B: Mechanical Engineering*, 5(4):041013 (12 pages), 2019.

Ferson, S., V. Kreinovich, L. Ginzburg, D. S. Myers and K. Sentz. *Constructing probability boxes and Dempster-Shafer structures*. Tech. Rep. SAND2002-4015, Sandia National Laboratories, 2003.

Freitag, S., P. Edler, K. Kremer, and G. Meschke. Multilevel surrogate modeling approach for optimization problems with polymorphic uncertain parameters. *International Journal of Approximate Reasoning*, 119:81–91, 2020.

Kennedy, J. and R. C. Eberhart. Particle Swarm Optimization. In *Proceedings of the IEEE International Conference on Neural Networks IV*, pp. 1942–1948, IEEE Press, Piscataway, 1995.

Lazarov, B. S., M. Schevenels, and O. Sigmund. Topology optimization with geometric uncertainties by perturbation techniques. *International Journal for Numerical Methods in Engineering*, 90:1321–1336, 2012.

Lin, B. and X. Li. The effect of carbon tax on per capita CO_2 emissions. *Energy Policy*, 39:5137–5146, 2011.

López, C., A. Baldomir, and S. Hernández. Deterministic versus reliability-based topology optimization of aeronautical structures. *Structural and Multidisciplinary Optimization*, 53:907–921, 2016.

Mäck, M., I. Caylak, P. Edler, S. Freitag, M. Hanss, R. Mahnken, G. Meschke, and E. Penner. Optimization with constraints considering polymorphic uncertainties. *GAMM-Mitteilungen (Surveys for Applied Mathematics and Mechanics)*, 42(1):e201900005, 1–12, 2019.

Naboni, R. and I. Paoletti. Architectural morphogenesis through topology optimization. In D. D'Uva, editor, *Handbook of Research on Form and Morphogenesis in Modern Architectural Contexts*, Chapter 4, pages 69–92. IGI Global, 2018.

París, J., S. Martínez, F. Navarrina, and M. Casteleiro. Topology optimization of aeronautical structures with stress constraints: general methodology and applications. *Proceedings of the Institution of Mechanical Engineers, Part G: Journal of Aerospace Engineering*, 226(5):589–600, 2012.

Schöbi, R. and B. Sudret. Structural reliability analysis for p-boxes using multi-level meta-models. *Probablistic Engineering Mechanics*, 48:27–38, 2017.

Schuëller, G. I. and H. A. Jensen. Computational methods in optimization considering uncertainties – An overview. *Computer Methods in Applied Mechanics and Engineering*, 198(1):2–13, 2008.

Sigmund, O. A 99 line topology optimization code written in Matlab. *Structural and Multidisciplinary Optimization*, 21:120–127, 2001.

Sigmund, O. and K. Maute. Topology optimization approaches. *Structural and Multidisciplinary Optimization*, 48(6):1031–1055, 2013.

Thore, C. J., E. Holmberg, and A. Klarbring. A general framework for robust topology optimization under load-uncertainty including stress constraints. *Computer Methods in Applied Mechanics and Engineering*, 319:1–18, 2017.

Valdebenito, M. A. and G. I. Schuëller. A survey on approaches for reliability-based optimization. *Structural and Multidisciplinary Optimization*, 42(5):645–663, 2010.

Wang, D. and W. Gao. Robust topology optimization under multiple independent uncertainties of loading positions. *International Journal for Numerical Methods in Engineering*, 121:4944–4970, 2020.